

Coordination polymers based on octacyanometalates(IV,V) (M = Mo, W) and aliphatic polyamine copper(II) tectons with [N₃] donor atom sets †

Robert Podgajny,^a Tomasz Korzeniak,^a Katarzyna Stadnicka,^a Yves Dromzée,^b Nathaniel W. Alcock,^c William Errington,^c Krzysztof Kruczała,^a Maria Bałanda,^d Terence J. Kemp,^c Michel Verdaguer^b and Barbara Sieklucka^{*a}

^a Faculty of Chemistry, Jagiellonian University, Ingardena 3, 30-060 Kraków, Poland

^b Laboratoire de Chimie Inorganique et Matériaux Moléculaires, Unité associée au C. N. R. S. 7071, Université Pierre et Marie Curie, 75252 Paris Cedex 05, France

^c Department of Chemistry, University of Warwick, Coventry, UK CV4 7AL

^d H. Niewodniczanski Institute of Nuclear Physics, Radzikowskiego 152, 31-342 Kraków, Poland

Received 6th June 2003, Accepted 21st July 2003

First published as an Advance Article on the web 1st August 2003

The cyano-bridged [Cu^{II}(tetrenH₂)₂][W^{IV}(CN)₈]₂·5H₂O (tetren = tetraethylenepentamine) (**1**), [Cu^{II}(tetrenH₂)-[Cu^{II}(tetrenH)]][W^V(CN)₈][W^{IV}(CN)₈]₂·2.5H₂O (**2**), [Cu^{II}(dien)]₂[W^{IV}(CN)₈]₂·4H₂O (dien = diethylenetriamine) (**3**) and its isomorphous molybdenum(IV) analogue (**4**) have been prepared and structurally characterised. **1** and **2** are built from the W₂Cu₂(μ-CN)₄ squares extended into 1-D structure by cyano-bridges. 2-D **3** and **4** form a square grid pattern with tungsten atoms in the corners and –CN–Cu(dien)–NC– linkages on the edges of the squares. The magnetic behaviour of **1** and **3** indicates the presence of two isolated Cu^{II} spins *S* = 1/2 with a very weak antiferromagnetic coupling through the diamagnetic NC–W^{IV}–CN bridges in the low temperatures. Assembly **2** exhibits a weak ferromagnetic interaction between Cu^{II} and W^V isolated by diamagnetic [W^{IV}(CN)₈]⁴⁻ spacer from another Cu^{II} centre within W^V–CN–Cu^{II}–NC–W^{IV}–CN–Cu^{II} unit and the antiferromagnetic interaction between the Cu^{II}₂W^VW^{IV} units.

Introduction

Coordination network structures based on octacyanometalates [M(CN)₈]³⁻⁴⁻ (M = Mo and W) and 3d metal centres have been one of the attractive subjects in crystal engineering of coordination polymers owing to their attractive new topologies, interesting structural features and potential applications as functional materials.¹ The design of such molecular architectures is based on the building block (tecton) approach in solution.² The topology of self-assembled coordination network is encoded into the individual building blocks due to their steric, topological and intermolecular bonding capabilities. Furthermore, the inherent coordination preferences of the metal cationic building blocks used in the assembly process are coupled with the stereochemical non-rigidity of the octacyanometalate moiety.³

As a part of our programme working towards the crystal engineering of coordination networks, the design and synthesis of octacyanometalate based assemblies involving M^{IV,V}–CN–Cu^{II} linkages is a major goal. The bare Cu(II) centres coordinate [Mo(CN)₈]³⁻ and [Mo(CN)₈]⁴⁻ to give the three-dimensional polymers of stoichiometries {Cu_{1.5}[Mo^V(CN)₈]₂·3H₂O}_{*n*}⁴ and Cu₂[Mo^{IV}(CN)₈]₂^{1h,4} respectively. The use of amine or polyamine blocking ligands at Cu^{II} leads to unique architectures: 1-D Cu₂(NH₃)₈[Mo^{IV}(CN)₈]₂⁵ 3-D {[Cu(en)₂]₃[W^V(CN)₈]₂·H₂O}_{*n*}^{ij} (en = ethylenediamine) and 3-D {[Cu(en)₂][Cu(en)][W^{IV}(CN)₈]₂·H₂O}_{*n*}^{1k} 1-D Na₃{[Cu^{II}(dien)]₄[W^V(CN)₈]₂·8H₂O}_{*n*}⁶ (dien = diethylenetriamine) or discrete 0-D [Cu(bpy)₂][Mo^{IV}(CN)₈]₂·5H₂O·CH₃OH.^{1h}

In order to explore the role of the coordination geometry along with the degree of chelation of cationic tectons in the self-assembly process, we have focused on the use of penta-coordinative tetren ligand (tetren = tetraethylenepentamine) at the Cu^{II} centre. Our strategy is based around the pH-dependent coordination of polyamine ligand in [Cu(tetren)]²⁺. We have successfully introduced this synthetic strategy in metal-directed supramolecular self-assembly of [W(CN)₈]³⁻ and [Cu(tetren)]²⁺ in acidic aqueous solution, which afforded the pre-programmed bare Cu(II) centres formed by release of fully protonated tetren ligand.⁷ The assembling units have produced the 2-D double-layered square grid polymer of {(tetrenH₅)_{0.8}Cu^{II}₄[W^V(CN)₈]₄·7.2H₂O}_{*n*}. The polymer contains Cu^{II} centres of square pyramidal geometry coordinatively saturated solely by CN bridges supplied by five [W(CN)₈]³⁻ ions and exhibits soft ferromagnetic behaviour with an ordering temperature *T*_C of 34 K.

We report here on the preparation, structures and physico-chemical characterization of the new series of bimetallic coordination polymers based on aliphatic polyamine copper(II) tectons with [N₃] donor atom sets and octacyanometalates: two 1-D [Cu^{II}(tetrenH₂)₂][W^{IV}(CN)₈]₂·5H₂O (**1**) and [Cu^{II}(tetrenH₂)-[Cu^{II}(tetrenH)]][W^V(CN)₈][W^{IV}(CN)₈]₂·2.5H₂O (**2**) and 2-D [Cu^{II}(dien)]₂[M^{IV}(CN)₈]₂·4H₂O [M = W (**3**), Mo (**4**)]. A preliminary account of (**3**) has been presented.⁸

Experimental

Materials

The precursors K₄[W^{IV}(CN)₈]₂·2H₂O,^{9a} K₄[Mo^{IV}(CN)₈]₂·2H₂O and Na₃[W^V(CN)₈]₂·4H₂O^{9b} were synthesized according to published procedures. The potassium salts were converted to appropriate Na⁺ salts using Dowex 50X 8 ion exchange resin. All reagents were of analytical grade and used without further purification. The synthetic procedures and all manipulation with Na₃[W^V(CN)₈]₂·4H₂O were carried out under red light in order to avoid photoreduction.¹⁰ The cationic precursors

† Electronic supplementary information (ESI) available: Tables S1 and S6 – The selected distances of possible hydrogen bonds in **3** and **1**. Tables S2–5 – Selected bond lengths and angles for **1–4**. Fig. S1 – Electronic spectra of [Cu^{II}(tetren)]²⁺ at different pHs. Fig. S2 – The dependence of the intensities of ν(CN) on the oxidation state of [W(CN)₈]^{*n*-}}. Fig. S3 – χ vs. *T* of 2·10.5H₂O and the best fit of the Curie–Weiss law. Inset: χ*T* vs. *T*. Fig. S4 – The ESR spectra of 1·3H₂O and 2·10.5H₂O. See <http://www.rsc.org/suppdata/dt/b3/b306422k/>

[Cu(tetren)](ClO₄)₂⁷ and [Cu^{II}(dien)₂Cl₂](ClO₄)₂¹¹ were prepared *via* a previously described procedure.

Synthesis of [Cu^{II}(tetrenH₂)₂][W^{IV}(CN)₈]₂·8H₂O, **1**·3H₂O

An equimolar mixture of CuCl₂·2H₂O (0.75 mmol, 0.128 g) and tetren·5HCl (0.75 mmol, 0.328 g) in 50 ml of water was neutralized to pH = 7 with NaOH and then a solution of Na₃[W^{IV}(CN)₈]₂·4H₂O (0.5 mmol, 0.267 g), neutralized to pH = 7, was added. The solution, after reduction in volume to ~5 ml was passed through a filled with silica gel column (50–100 mesh, Merck) and eluted with 100 ml of water. Two fractions were separated. The first, yellow fraction, was identified by its UV-vis spectrum as a salt of [W^{IV}(CN)₈]⁴⁻. The second, blue fraction afforded blue well-shaped prismatic crystals after the solvent was evaporated at room temperature for a few weeks. Yield: 0.0403 g, 12%. Anal. Calc. for C₃₂H₆₆W₂Cu₂O₈N₂₆: C, 26.7; N, 25.3; H, 4.6. Found: C, 27.2; N, 25.4; H, 4.6%. IR spectrum: ν(C≡N) (in cm⁻¹) 2160, 2151, 2128, 2107, 2101, 2095; ν(W–C) 604, 570; ν(Cu–N) 483; ν(OH) 3578; ν(NH) 3430, 3253, 3186; ν(CH) 2972, 2932; δ(NH) 1612; δ(CH₂) 1463, 1449; ν(C–N, C–C), δ(CH) 1395, 1373, 1315, 1255, 1224, 1204, 1146, 1120, 1110, 1082, 1075, 1014, 998, 934; γ(NH) 849, 861, 775 cm⁻¹.

1·3H₂O can be also obtained by reaction of Na₄[W^{IV}(CN)₈] (0.15 mmol, 15 ml) and [Cu^{II}(tetren)](ClO₄)₂ (0.3 mmol, 0.136 g, 452 g mol⁻¹, 20 ml) in aqueous solution at pH = 3.5 (HClO₄). Yield: 0.16 g, 48%. Anal. Calc. for C₃₂H₆₆W₂Cu₂O₈N₂₆: C, 26.7; N, 25.3; H, 4.6. Found: C, 27.1; N, 25.1; H, 4.0%. The blue crystals were grown by slow evaporation of solvent at room temperature. The single crystals of **1** obtained by both procedures were found to be isomorphous by X-ray analysis.

Synthesis of [Cu^{II}(tetrenH₂)][Cu^{II}(tetrenH)][W^{IV}(CN)₈]-[W^{IV}(CN)₈]₂·13H₂O, **2**·10.5H₂O

Aqueous solutions of Na₃[W^{IV}(CN)₈]₂·4H₂O (0.2 mmol, 0.107 g, 533 g mol⁻¹, 20 ml) and [Cu^{II}(tetren)](ClO₄)₂ (0.3 mmol, 0.136 g, 452 g mol⁻¹, 20 ml) at pH = 3.5 (HClO₄) were mixed together. After a few days a dark blue polycrystalline precipitate started to appear. After three weeks the precipitate was washed with water and dried in air. Yield: 0.15 g, 54%. Anal. Calc. for C₃₂H₇₅W₂Cu₂O₁₃N₂₆ (2·10.5H₂O): C, 25.2; N, 23.8; H, 5.0. Found: C, 25.5; N, 23.4; H, 4.2%. Dark blue prismatic crystals of **2** were grown by slow diffusion of the precursor complexes in aqueous solutions at pH 3.5 (HClO₄) in an H-tube over a period of 4 weeks. IR spectrum: ν(C≡N) 2156, 2143, 2115; ν(W–C) 610, 578; ν(Cu–N) 483; ν(OH) 3563; ν(NH) 3431, 3249; ν(CH) 2935; δ(NH) 1615; δ(CH₂) 1503, 1464; ν(C–N, C–C), δ(CH) 1332, 1315, 1223, 1120, 1076; ν(NH) 861, 776 cm⁻¹.

Synthesis of [Cu^{II}(dien)₂][W^{IV}(CN)₈]₂·4H₂O, **3**

To a stirred glycerol–water solution (1 : 2 v/v) of Na₄[W^{IV}(CN)₈] (0.2 mmol, 20 ml), a glycerol–water solution (1 : 2 v/v) solution of [Cu^{II}(dien)₂Cl₂](ClO₄)₂ (0.1 mmol, 20 ml, pH *ca.* 5.5) was slowly added. Well-shaped olive-green needle-like crystals were grown by slow evaporation at room temperature. The crystals were washed with water and dried in air. Yield: 0.121 g, 76%. Anal. Calc. for [Cu^{II}(dien)₂][W^{IV}(CN)₈]₂·4H₂O: C, 24.1; N, 24.6; H, 4.3. Found: C, 24.0; N, 24.5; H, 3.8%. IR spectrum: ν(C≡N) 2157, 2131, 2112; ν(W–C) 507; ν(Cu–N) 468; ν(OH), 3445; ν(NH) 3428, 3331, 3235; ν(CH) 2956, 2883; δ(NH) 1641, 1587; δ(CH₂) 1464, 1448; ν(C–N, C–C), δ(CH) 1391, 1322, 1285, 1256, 1138, 1093, 1025; γ(NH) 898, 873 cm⁻¹.

Synthesis of [Cu^{II}(dien)₂][Mo^{IV}(CN)₈]₂·4H₂O, **4**

The procedure was analogous to that of **3**: glycerol–water solution (1 : 2 v/v) of Na₄[Mo^{IV}(CN)₈] (0.2 mmol, 20 ml) was used. Yield: 0.0832 g, 58%. Anal. Calc. for [Cu^{II}(dien)₂][Mo^{IV}(CN)₈]₂·4H₂O: C, 27.1; N, 27.6; H, 4.8. Found: C, 26.8; N, 27.8; H,

4.6%. The IR spectrum is identical to that of [Cu^{II}(dien)₂][W^{IV}(CN)₈]₂·4H₂O.

Physical measurements

IR spectra of the assemblies **1–4** were recorded between 4000–400 cm⁻¹ in KBr pellets using a Bruker IFS 47 spectrometer. Electronic spectra were recorded using a Shimadzu 2101 PC spectrophotometer. ESR spectra of **1** and **2** at X band were measured at ambient and liquid nitrogen (77 K) temperatures with Bruker EPS-500 (ELEXSYS) spectrometer operating at 9.7 GHz and 100 kHz modulation. ESR spectra were simulated with the program SIM-14A.¹² Magnetic measurements of **1–3** were carried out with a 7227 Lake Shore AC Susceptometer/DC Magnetometer in the temperature range 4.2–200 K. Diamagnetic corrections were made using Pascal's constants. Measurements of pH were performed with a ELMETRON CP-315M pH meter with an ELMETRON OS 10-10 electrode.

Determination of distribution pattern of pH-dependent chelation forms of [Cu(tetren)](ClO₄)₂

The electronic visible spectra of [Cu(tetren)](ClO₄)₂ of concentration 3.077·10⁻³ M were measured in the pH range 1 < pH < 13. Buffer solutions were made of 0.4 M HClO₄–0.4 M NaClO₄ (pH 1–7) and 0.4 M NaOH–0.4 M NaClO₄ (pH 7–13). The ionic strength was kept constant at *I* = 0.4 M (NaClO₄). Measurements were carried out at a constant temperature of 25 °C. Computations were performed using program SPECFIT.¹³

Crystallographic data collection and structure determination

Crystallographic data and details of the refinements are collected in condensed form in Table 1.

The crystal data for [Cu^{II}(tetrenH₂)₂][W^{IV}(CN)₈]₂·5H₂O, **1**, were collected using an Enraf-Nonius CAD4 diffractometer. No significant variations were observed in the intensities of two checked reflections during data collections. Absorption corrections were applied using the *ψ* scan method. The structure was solved with SHELXS-86¹⁴ followed by Fourier maps techniques and refined by full matrix least squares with anisotropic thermal parameters for all non-hydrogen atoms. Refinement was performed using the PC version of Crystals.¹⁵ Scattering factors and corrections for anomalous dispersion were taken from Cromer.¹⁶

The crystal structure of [Cu^{II}(tetrenH₂)][Cu^{II}(tetrenH)][W^{IV}(CN)₈][W^{IV}(CN)₈]₂·2.5H₂O, **2**, was determined using a Siemens SMART diffractometer three-circle system with a CCD area detector. The structure was solved by direct methods using SHELXS-90 (TREF) with additional light atoms found by Fourier methods. The lattice includes extensive solvent molecules, modelled as five oxygen atoms (all with 0.5 occupancy). Hydrogen atoms on the terminal nitrogen atoms of the tetren molecules and on the solvent molecules were not included. Other hydrogen atoms were added at calculated positions and refined using a riding model. Anisotropic displacement parameters were used for all non-H atoms apart from the solvent atoms; H-atoms were given isotropic displacement parameters equal to 1.2 times the equivalent isotropic displacement parameter of the atom to which the H-atom is attached. The platy crystals diffracted weakly and the relatively high *R* value is to be expected; the small number of peaks in the final difference Fourier synthesis higher than 1 e Å⁻³ are all close to the tungsten atoms.

Intensity data for [Cu^{II}(dien)₂][W^{IV}(CN)₈]₂·4H₂O, **3**, and [Cu^{II}(dien)₂][Mo^{IV}(CN)₈]₂·4H₂O, **4**, were collected on a single crystal diffractometer Nonius Kappa CCD¹⁷ using a graphite-monochromated MoK α radiation (λ = 0.71073 Å). No crystal decay was observed. Absorption corrections were applied using multi-scan method DENZO.¹⁸ The structures were solved with the SIR¹⁹ and refined with SHELXL programs.²⁰

Table 1 Crystal data for the assemblies 1, 2, 3 and 4

	1	2	3	4
Empirical formula	C ₃₂ H ₆₀ W ₂ Cu ₂ O ₅ N ₂₆	C ₃₂ H ₅₅ W ₂ Cu ₂ O _{2.5} N ₂₆	C ₁₆ H ₃₄ WCu ₂ O ₄ N ₁₄	C ₁₆ H ₃₄ MoCu ₂ O ₄ N ₁₄
Formula weight	1383.7	1338.7	797.50	709.59
Crystal system, space group	Triclinic, <i>P</i> $\bar{1}$	Triclinic, <i>P</i> $\bar{1}$	Orthorhombic, <i>P</i> ₂ ₁ ₂ ₁ ²	Orthorhombic, <i>P</i> ₂ ₁ ₂ ₁ ²
<i>a</i> /Å	14.675(2)	11.0223(6)	12.8799(1)	12.8722(2)
<i>b</i> /Å	15.215(2)	16.6418(9)	9.9690(2)	9.97630(10)
<i>c</i> /Å	16.074(2)	17.6382(10)	11.3691(2)	11.3757(2)
<i>a</i> °	62.54(1)	75.920(3)	90	90
<i>β</i> °	63.44(1)	77.685(3)	90	90
<i>γ</i> °	62.02(1)	71.825(3)	90	90
<i>V</i> /Å ³	2687.6(8)	2948.3(3)	1459.79(4)	1460.83(4)
<i>Z</i>	2	2	2	2
<i>T</i> /K	295	180(2)	293(2)	293(2)
μ (MoK α)/mm ⁻¹	5.20	4.651	5.421	1.913
Reflections collected	9892	15096	10623	6352
Unique reflections, <i>R</i> _{int}	9438, 0.0454	10085, 0.0621	10623, 0.00	6352, 0.00
Observed reflections	7391 [<i>I</i> > 3 σ (<i>I</i>)]	7897 [<i>I</i> > 2 σ (<i>I</i>)]	9058 [<i>I</i> > 2 σ (<i>I</i>)]	5848 [<i>I</i> > 2 σ (<i>I</i>)]
Final <i>R</i> ₁ / <i>wR</i> ₂	0.0604/0.0695	0.0959/0.2203	0.0347/0.0735	0.0355/0.0824

The investigated crystals of **3** exhibited twinning described by the twin matrix $-1\ 0\ 0 / 0\ -0.491\ -0.764 / 0\ -0.994\ 0.491$ (180° rotation about the [0, -2, 3] direction) and the twin component factor was refined to 0.402(10). The position of hydrogen atoms of (CH₂)₂ in the dien ligand were calculated using geometrical constraints and included in the refinement using a riding model. Because of the ligand disorder we were unable to estimate the position of the hydrogen atoms at amine nitrogens. The hydrogen atoms of water molecules were also not found, but the inspection of a close vicinity of the oxygen atoms shows that O1 as well as O2 could be considered as water oxygen due to the possible formation the hydrogen bonds to two N atoms of cyano ligands (Table S1 †).

The investigated crystals of **4** exhibited twinning described by the twin matrix $-1\ 0\ 0 / 0\ -1\ 0 / 0\ 0\ -1$ and the twin component factor was refined to 0.557(13). To describe the disorder of dien ligand, a libration of the ligand in the equatorial plane of [Cu(dien)(NC)₂] moiety was assumed. Therefore the external positions of C and N atoms of dien were refined in the isotropic approximation. The positions of hydrogen atoms were calculated from geometrical constraints and included in the refinement in a riding model. Compound **4** was found to be isomorphous with compound **3**.

CCDC reference numbers 203323–203325 and 212730.

See <http://www.rsc.org/suppdata/dt/b3/b306422k/> for crystallographic data in CIF or other electronic format.

Results and discussion

Characterization of cationic precursors and design principles

To explore the role of the coordination geometry along with the degree of chelation of cationic tectons in the self-assembly process, we investigated the self assembly of aliphatic polyamine copper(II) tectons with [N₃] donor atom sets together with octacyanometalates(IV,V) precursors. Our strategy arises from the pH-dependent coordination of the polyamine ligand in the [Cu(tetren)]²⁺ complex.

The crystal structure analysis of the [Cu(tetren)](ClO₄)₂ precursor⁷ revealed that [Cu(tetren)]²⁺ cation in the crystal lattice favours trigonal bipyramidal geometry (TBP) over the square-pyramidal (SP) structure. The [Cu(tetren)]²⁺ complex of distorted TBP geometry has significantly longer terminal equatorial Cu–N bonds compared to the remaining central Cu–N bonds. The geometry of the coordinatively saturated [Cu(tetren)]²⁺ precursor implies that the terminal N–Cu bonds would be the first to be detached in the pH-dependent coordination of the tetren ligand as well as in the self-assembly process in favour of cyano bridges.

Fig. 1 presents the three-dimensional diagram of visible electronic spectra of [Cu(tetren)](ClO₄)₂ vs. pH in aqueous

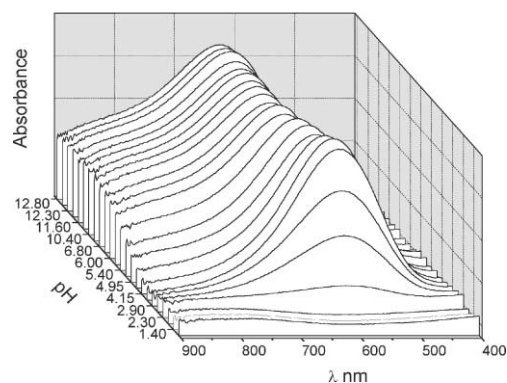


Fig. 1 Three-dimensional presentation of visible electronic spectra of [Cu(tetren)](ClO₄)₂ complex at different pHs.

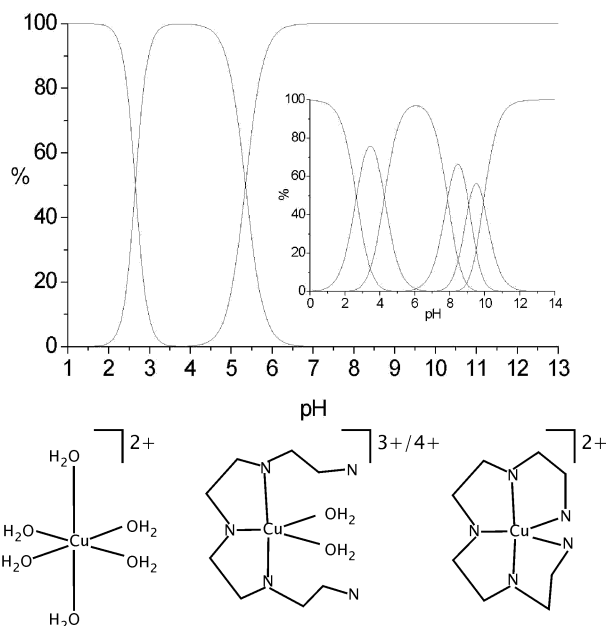
solution. The spectra are dependent on the coordination geometry of the Cu^{II}N₅ centre^{21,22} as well as indicating the pH-dependent coordination of the polyamine ligand.^{23,24} Comparison with visible electronic spectra of the CuN₅, CuN₃O₂ and [Cu(H₂O)₆]²⁺ chromophores (Table 2, Fig. S1 †) enables us to draw qualitative conclusions. In alkaline and neutral solutions, the [Cu(tetren)]²⁺ ion exhibits a main band at 630 nm and a shoulder at 840 nm indicative of square-pyramidal coordination in aqueous solution.^{21,22,25} In more acidic solutions, the main band at 590 nm is very similar in shape and energy to that reported for the CuN₃O₂ chromophore of SP geometry in [Cu(dien)(H₂O)₂]²⁺²² and can be attributed to [N₃] coordination of tetren to the Cu(II) centre. In strongly acidic solutions very weak complex asymmetric d–d absorption bands above 800 nm are observed, which are characteristic of [Cu(H₂O)₆]²⁺.²⁶

The distribution pattern of [Cu(tetren)]²⁺ pH-dependent chelation forms was established from the electronic spectra by using the model-free Evolving Factor Analysis (Fig. 2). The [Cu(tetren)]²⁺ is the single source of pre-programmed Cu^{II} centres formed by the dechelation of the N atoms of tetren ligand. [Cu(tetren)]²⁺ exists at pH > 6. In the pH range 3–5, [Cu^{II}(tetrenH₂)(H₂O)₂]⁴⁺ and/or [Cu^{II}(tetrenH)(H₂O)₂]³⁺²⁷ (indistinguishable by the numerical procedure employed) with [N₃] coordination of tetren, are formed. At pH < 2, the release of the fully protonated tetren ligand leads to [Cu(H₂O)₆]²⁺. The distribution pattern of the chelation forms of [Cu(tetren)]²⁺ can be compared to that of the protonation forms of the free tetren ligand (Fig. 2, inset), which gives rise to tetrenH₅⁵⁺, tetrenH₄⁴⁺, tetrenH₃³⁺, tetrenH₂²⁺, tetrenH⁺ and tetren species with increasing pH.²⁸

Taking into account the distribution pattern of the protonation forms of [Cu(tetren)]²⁺, syntheses at pHs 7.0 and 3.5 were carried out, for which we observed [Cu(tetren)]²⁺ and [Cu^{II}(tetrenH₂)(H₂O)₂]⁴⁺ as the dominating species, respectively.

Table 2 Electronic spectra of $[\text{CuN}_3]^{2+}$, $[\text{CuN}_3(\text{H}_2\text{O})_2]^{4+}$ and $[\text{Cu}(\text{H}_2\text{O})_6]^{2+}$ chromophores in the ligand-field (LF) range

Complex	LF bands/nm	Geometry	Ref.
$[\text{Cu}(\text{tren})]^{2+}$	630, 820(sh)	SP	This work, pH > 5.5
$[\text{Cu}(\text{NH}_3)_5]^{2+}$	654, 909(sh)	SP	21, 25
$[\text{Cu}(\text{tren})\text{L}]^{2+}$ L = 4,5-diazafluoren-9-one	621, 813(sh)	SP	22
$[\text{Cu}(\text{tren})\text{L}]^{2+}$ L = ImH	662(sh), 806	TBP	22
$[\text{Cu}(\text{tren})\text{L}]^{2+}$ L = NH_3	657(sh), 877	TBP	21
$[\text{Cu}(\text{trenH}_2)(\text{H}_2\text{O})_2]^{4+}$	590	SP	This work, 2.5 < pH < 5.5
$[\text{Cu}(\text{dien})(\text{H}_2\text{O})_2]^{2+}$	614	SP	24
$[\text{Cu}(\text{H}_2\text{O})_6]^{2+}$	800	Axially distorted octahedron, D_{4h}	This work, pH < 2.5, 26

**Fig. 2** The distribution pattern (top) and schematic presentation (bottom) pH-dependent chelation forms of $[\text{Cu}(\text{tren})]^{2+}$. Inset in the top figure: distribution pattern of tren protonation forms.

Setting the initial pH to 7.0, the self-assembly of coordinatively saturated $[\text{Cu}(\text{tren})]^{2+}$ units together with $[\text{W}(\text{CN})_8]^{3-}$ affords $[\text{Cu}^{\text{II}}(\text{trenH}_2)_2][\text{W}^{\text{IV}}(\text{CN})_8]_2 \cdot 8\text{H}_2\text{O}$, $1 \cdot 3\text{H}_2\text{O}$. At pH 3.5, $[\text{Cu}^{\text{II}}(\text{trenH}_2)(\text{H}_2\text{O})_2]^{4+}$ assembles with $[\text{W}^{\text{V}}(\text{CN})_8]^{3-}$ to give $[\text{Cu}^{\text{II}}(\text{trenH}_2)][\text{Cu}^{\text{II}}(\text{trenH})][\text{W}^{\text{V}}(\text{CN})_8] \cdot [\text{W}^{\text{IV}}(\text{CN})_8] \cdot 13\text{H}_2\text{O}$, $2 \cdot 10.5\text{H}_2\text{O}$. The analytical, spectroscopic and magnetic data (see below) for $1 \cdot 3\text{H}_2\text{O}$ and $2 \cdot 10.5\text{H}_2\text{O}$ clearly indicate the reduction of $[\text{W}^{\text{V}}(\text{CN})_8]^{3-}$ to $[\text{W}^{\text{IV}}(\text{CN})_8]^{4-}$. The partial reduction of W(v) and the presence of both $[\text{W}^{\text{IV}}(\text{CN})_8]^{4-}$ and $[\text{W}^{\text{V}}(\text{CN})_8]^{3-}$ in $2 \cdot 10.5\text{H}_2\text{O}$ is suggested by quantitative analysis of magnetic susceptibility data. The proposed formula of $2 \cdot 10.5\text{H}_2\text{O}$ is confirmed by the formation of $1 \cdot 3\text{H}_2\text{O}$ by the assembly of $[\text{Cu}^{\text{II}}(\text{trenH}_2)(\text{H}_2\text{O})_2]^{4+}$ with $[\text{W}^{\text{IV}}(\text{CN})_8]^{4-}$ at pH 3.5, which would otherwise produce $2 \cdot 10.5\text{H}_2\text{O}$. The mechanism of the observed reduction of $[\text{W}^{\text{V}}(\text{CN})_8]^{3-}$ to $[\text{W}^{\text{IV}}(\text{CN})_8]^{4-}$ seems to be complex and the phenomenon may be similar to that observed in several $[\text{Fe}^{\text{III}}(\text{CN})_6]^{3-}$ -Cu(II) extended and discrete compounds.²⁹⁻³¹

The reaction of $[\text{Cu}(\text{dien})(\text{H}_2\text{O})_2]^{2+}$ tecton containing an analogous tridentate blocking ligand with $[\text{M}(\text{CN})_8]^{4-}$ generates $[\text{Cu}^{\text{II}}(\text{dien})_2][\text{M}^{\text{IV}}(\text{CN})_8] \cdot 4\text{H}_2\text{O}$ (3 and 4).

In our approach, the aliphatic polyamine copper(II) tectons with $[\text{N}_3]$ donor atom sets capable of forming moieties with different coordination numbers and geometries assemble together with octacyanometalates into the required geometrical orientations to form unique cyano-bridged coordination polymers stabilised by H-bonding interactions.

Supramolecular crystal structures of bimetallic assemblies

$[\text{Cu}^{\text{II}}(\text{trenH}_2)_2][\text{W}^{\text{IV}}(\text{CN})_8]_2 \cdot 5\text{H}_2\text{O}$, **1**. The structure of the assembly consists of 1-dimensional chains of a necklace pattern

built of two different types of $\text{W}_2\text{Cu}_2(\mu\text{-CN})_4$ squares joined alternately by cyano bridges (Fig. 3a) together with water of crystallization. Selected bond distances and angles are collected in Table 3.

The essential difference between the two W units is related to their connectivity with the Cu centres (Fig. 3b): the W(1) centre of distorted dodecahedral geometry forms three cyano bridges, while the W(2) centre of almost ideal dodecahedral geometry forms two cyano bridges. The W-C-N angles are almost perfectly linear with a mean value of 178.0° and maximum deviation from linearity of 4.6° . The mean values of W-C and C-N bonds lengths are 2.17 and 1.13 Å, respectively, which are typical for cyano-bridged assemblies based on octacyanometalates.^{1e,m,3,5,32}

The copper units also differ significantly: Cu(1) has a square pyramidal geometry, while Cu(2) has a strongly axial distorted octahedral geometry.

The pentacoordinate Cu(1) centre contains three nitrogen donor atoms of the trenH_2 ligand in the square plane with bond lengths and angles in $[\text{Cu}(\text{I})(\text{trenH}_2)]^{4+}$ fragment (the average Cu-N_{tren} distances are close to 2 Å) typical for Cu-polyamine complexes,^{5,21,25,33-35} whereas two terminal N atoms (N31 and N35) of tren are not bound. The 5-coordination of the Cu(1) centre in $[\text{Cu}(\text{I})(\text{trenH}_2)(\text{NC})_2]^{2+}$ is completed by two N-donors of CN bridges from neighbouring W(1) centres.

The Cu(1)-N_{NC}-C linkages show different geometries: being short when coordinated in the equatorial position of copper [Cu(1)-N(14), 1.977(9) Å], but significantly longer at the axial position of the pyramidal Cu centre [Cu(1)-N(11), 2.183(9) Å]. The resulting distances between W and Cu in the W(1)-C-N_{NC}-Cu(1) entities are alternately short (5.262 Å) and long (5.327 Å). These two sets of distances are related to two different nonlinear geometries of the W(1)-C-N_{NC}-Cu(1) unit: being less bent in the equatorial short CN bridge [Cu(1)-N(14)-C(14), $171.1(8)^\circ$] and significantly more bent in the axial long CN bridge [Cu(1)-N(11)-C(11), $154.3(8)^\circ$]. The metric parameters of $[\text{Cu}(\text{I})(\text{trenH}_2)(\text{NC})_2]$ are in good agreement with other cyano bridged compounds containing the $[\text{Cu}(\text{dien})(\text{NC})_2]$ moiety: $[\text{Cu}(\text{dien})]_3[\text{Fe}(\text{CN})_6]_2 \cdot 6\text{H}_2\text{O}$,³³ $\{[\text{Cu}(\text{dien})]_2\text{-Cr}(\text{CN})_6\}_n[\text{Cu}(\text{dien})(\text{H}_2\text{O})\text{Cr}(\text{CN})_6]_n \cdot 4n\text{H}_2\text{O}$.³⁴

The Cu(2) centre coordinates three CN⁻ bridges to give the *mer*- $[\text{Cu}(\text{II})(\text{trenH}_2)(\text{NC})_3]^+$ moiety which has an elongated octahedral geometry. The two terminal N atoms (N41 and N45) of the trenH_2 ligand are not bound, whereas the other three nitrogen donor atoms of the trenH_2 are coordinated in the square plane with typical bond lengths and angles. The *mer*- $[\text{Cu}(\text{II})(\text{trenH}_2)(\text{NC})_3]^+$ features three distinct Cu(2)-N_{NC}-C linkages: two long [Cu(2)-N(12), 2.266(9) Å; Cu(2)-N(28b), 2.820 Å] and strongly bent [Cu(2)-N(12)-C(12), $146.5(8)^\circ$; Cu(2)-N(28b)-C(28b), 148.57°] [symmetry operation: (b) $-x, -y, -z + 2$] W(2)-C-N_{NC}-Cu(2) entities occupy the axial positions, whereas the equatorial bridge is shorter (Cu(2)-N(21), 1.960(8) Å) and almost linear [Cu(2)-N(21)-C(21), $175.8(9)^\circ$]. The relatively long Cu(2)-N(28b) bond can be interpreted in terms of a weak coordination bond, as long as the position of the N28 atom allows the *mer*- $[\text{Cu}(\text{II})(\text{trenH}_2)(\text{NC})_3]^+$ unit to maintain an approximately octahedral geometry. The almost identical coordination was observed in the hexa-coordinated

Table 3 Selected bond lengths (Å) and angles (°) for $[\text{Cu}^{\text{II}}(\text{tetrenH}_2)]_2[\text{W}^{\text{IV}}(\text{CN})_8]_2 \cdot 5\text{H}_2\text{O}$, **1**, and $[\text{Cu}^{\text{II}}(\text{tetrenH}_2)][\text{Cu}^{\text{II}}(\text{tetrenH})][\text{W}^{\text{V}}(\text{CN})_8][\text{W}^{\text{IV}}(\text{CN})_8] \cdot 2.5\text{H}_2\text{O}$, **2**

$[\text{Cu}^{\text{II}}(\text{tetrenH}_2)]_2[\text{W}^{\text{IV}}(\text{CN})_8]_2 \cdot 5\text{H}_2\text{O}$, **1**

$[\text{W}(1)(\text{CN})_8]^{4-}$ and $[\text{W}(2)(\text{CN})_8]^{4-}$

W1–C range/W1–C _{av.}	2.15–2.19/2.17	C–N range/C–N _{av.}	1.10–1.17/1.14	W1–C–N range	176.6–178.7
W2–C range/W2–C _{av.}	2.15–2.19/2.17	C–N range/C–N _{av.}	1.11–1.15/1.13	W2–C–N range	175.4–179.6

$[\text{Cu}(1)(\text{tetrenH}_2)(\text{NC})_2]^{2+}$

$\text{mer-}[\text{Cu}(2)(\text{tetrenH}_2)(\text{NC})_3]^+$

Cu1–N14	1.977(9)	Cu1–N14–C14	171.1(8)	Cu2–N21	1.960(8)	Cu2–N21–C21	175.8(9)
Cu1–N11	2.183(9)	Cu1–N11–C11	154.3(8)	Cu2–N12	2.266(9)	Cu2–N12–C12	146.5(8)
				Cu2–N28a	2.82	Cu2–N28a–C28a	148.6

$[\text{Cu}^{\text{II}}(\text{tetrenH}_2)][\text{Cu}^{\text{II}}(\text{tetrenH})][\text{W}^{\text{V}}(\text{CN})_8][\text{W}^{\text{IV}}(\text{CN})_8] \cdot 2.5\text{H}_2\text{O}$, **2**

$[\text{W}(1)(\text{CN})_8]^{4-}$ and $[\text{W}(2)(\text{CN})_8]^{4-}$

W–C range/W–C _{av.}	2.11–2.19/2.16	C–N range/C–N _{av.}	1.11–1.17/1.14	W1–C–N range	173.4–179
------------------------------	----------------	------------------------------	----------------	--------------	-----------

$\text{mer-}[\text{Cu}(3)(\text{tetrenH}_2)(\text{NC})_3]^+$

$\text{mer-}[\text{Cu}(4)(\text{tetrenH}_2)(\text{NC})_3]^+$

Cu3–N11	1.971(17)	Cu3–N11–C11	167.1(14)	Cu4–N12	1.944(19)	Cu4–N12–C12	172.1(17)
Cu3–N16a	2.431(18)	Cu3–N16a–C16a	149.6(16)	Cu4–N22	2.287(16)	Cu4–N22–C22	149.9(18)
Cu3–N18b	2.446(16)	Cu3–N18b–C18b	175.2(19)	Cu4–N28c	3.114(19)	Cu4–N28c–C28c	148.4

Symmetry equivalent operation for **1**: (a) $-x, -y, -z + 2$. Symmetry equivalent operations for **2**: (a) $1 - x, -y, 1 - z$; (b) $x - 1, -y, -z + 1$; (c) $x - 1, y, z$; the numbers given without the esd values have been read directly from ORTEP.

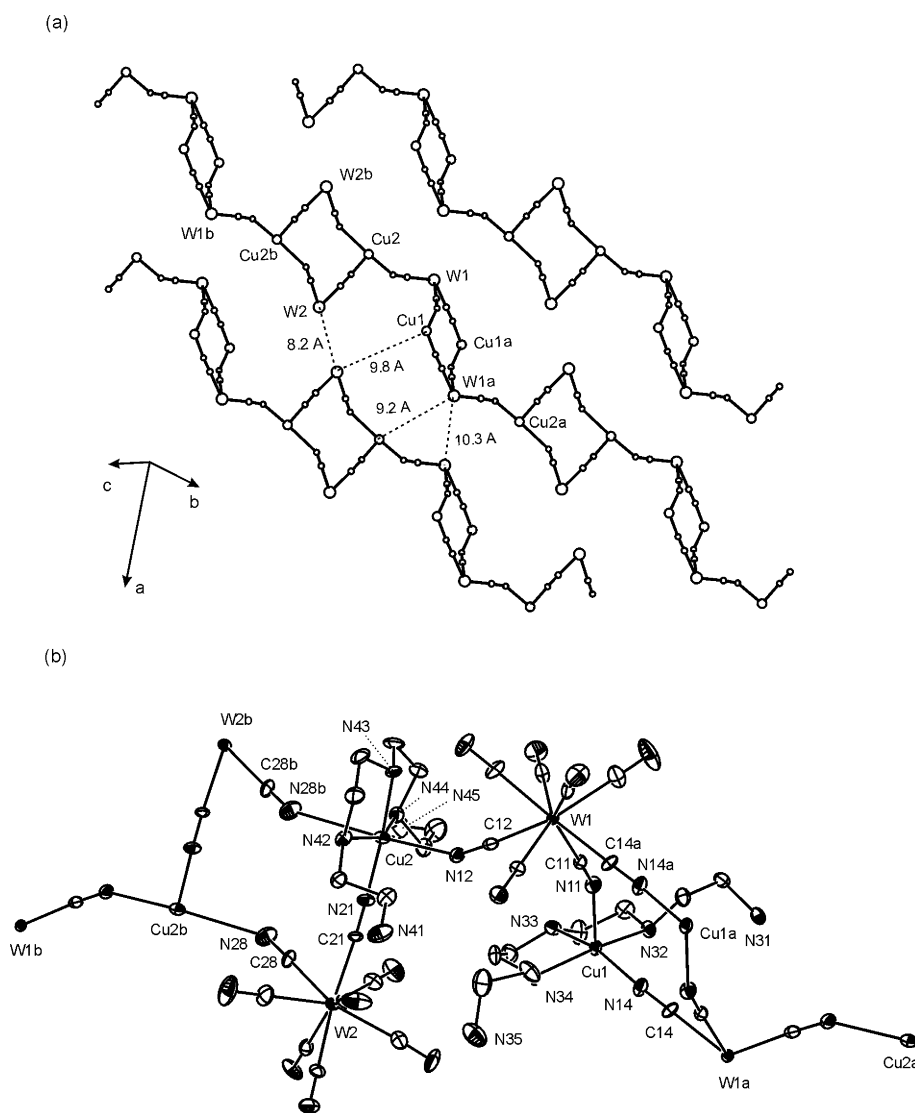


Fig. 3 Crystal structure of **1**: (a) skeletal view of cyano-bridged chain (only W(IV), Cu(II) centres and the CN^- bridging ligands are shown), (b) an ORTEP drawing, in which selected atoms are numbered, showing cyano-bridged W_2Cu_2 units [symmetry equivalent operation: (a) $-x, -y, -z + 2$]. All atoms are represented by 30% probability ellipsoids. Hydrogen and oxygen atoms are omitted for clarity.

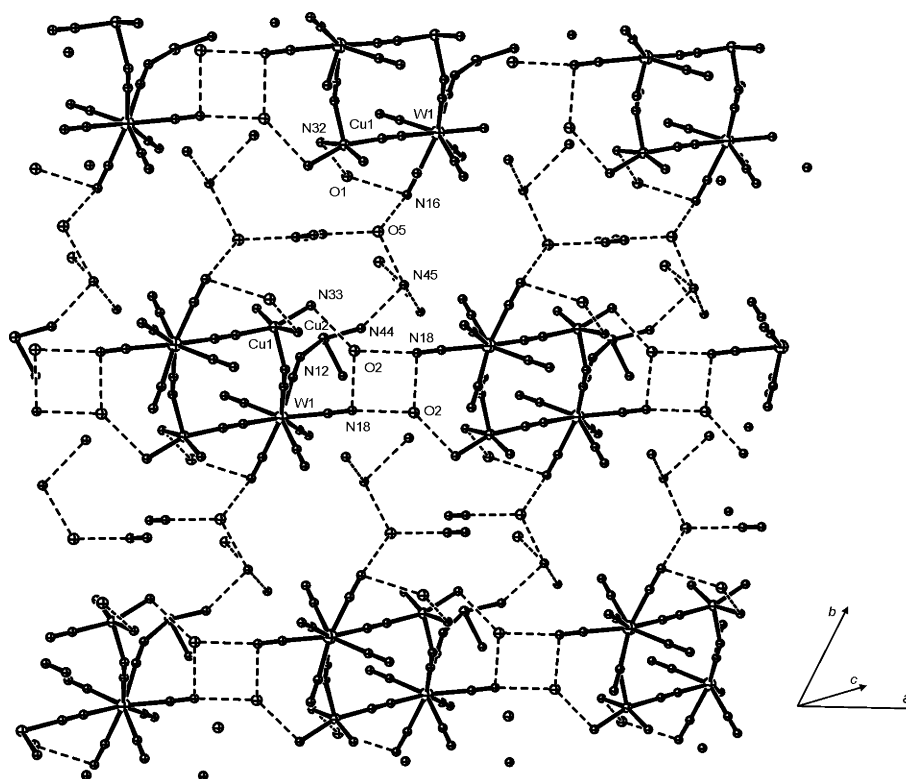


Fig. 4 ORTEP drawing exhibiting the selected hydrogen bonds connections between square W_2Cu_2 units in **1**. C and N atoms of tetren ligand are omitted for clarity.

$[Cu(tren)L]^{2+}$ (L = bidentate ligand 4,5-diazafluoren-9-one), which has average equatorial C–N bond lengths of 2.035 Å and axial C–N bond lengths of 2.244 and 2.995 Å.²² Similarly, in the 3-D compound $[Cu(en)_2][W(CN)_8]_2$, the Cu–N distances of the axially coordinated cyano-bridges fall within the range 2.33–2.73 Å.¹⁷ The terminal amino groups of tetrenH₂, terminal cyano ligands and water molecules are involved in a hydrogen bond network, stabilizing the 3-D supramolecular architecture (Fig. 4, Table S6†).

$[Cu^{II}(tetrenH_2)][Cu^{II}(tetrenH)][W^{IV}(CN)_8][W^{IV}(CN)_8] \cdot 2.5H_2O$, **2**. The $[Cu^{II}(tetrenH_2)][Cu^{II}(tetrenH)][W^{IV}(CN)_8][W^{IV}(CN)_8] \cdot 2.5 H_2O$ assembly forms a unique 1-D chain resembling a three-row ribbon (Fig. 5a) almost parallel to the (011) crystallographic plane orientation. The ribbon features $Cu(3)_2W(1)_2$ fused squares forming the central row and $Cu(3)Cu(4)_2W(1)_2W(2)$ distorted rectangles forming two external rows. Fig. 5b presents the local environment of the constituents of the compound. Selected bond lengths and angles are given in Table 3.

The W centres adopt a distorted square antiprismatic structure. Again, the main difference between the two W units is related to their connectivity with Cu centres as they possess very similar metric parameters: the W(1) centre forms four cyano bridges (two bridges originate from the opposite corners of the one square of SAP and the remaining two come from the neighbouring corners of the other square of SAP), while the W(2) centre forms two cyano-bridges (the bridging ligands originate from the opposite corners of one square of SAP). The mean W–C and C–N distances are 2.16 and 1.14 Å, respectively. The W–C–N bonds are almost linear with the angles in range 173.4–179°. The metric parameters of $[W(CN)_8]^{4-}$ and $[W(CN)_8]^{3-}$ are practically identical^{1e,m-o,3,5,7,32,36} and therefore cannot be diagnostic in determination of the oxidation state of the tungsten centre.

In **2**, the *mer*- $[Cu(tetrenH_2)(NC)_3]^+$ or *mer*- $[Cu(tetrenH)(NC)_3]$ moiety has the geometry of a strongly distorted, axially elongated octahedron. Three nitrogen donor atoms of tetrenH₂²⁺ or tetrenH⁺ are coordinated in the square plane with

typical bond lengths and angles, whereas the two terminal N atoms [N31, N35 in Cu(3) and N41, N45 (strongly delocalised) in Cu(4)] of tetren are not bound. The hexacoordinated Cu(3) moiety in the $W(1)_2Cu(3)_2$ subunit features shorter, bent equatorial bridges [Cu(3)–N(11), 1.971(17) Å; Cu(3)–N(11)–C(11), 167.1(14)°] and two longer, axial cyano bridges: strongly bent [Cu(3)–N(16a), 2.431(18) Å; Cu(3)–N(16a)–C(16a), 149.6(16)°] and almost linear [Cu(3)–N(18b), 2.446(16) Å; Cu(3)–N(18b)–C(18b), 175.2(19)°] [symmetry operations: (a) $-x, -y, 1-z$; (b) $-x-1, -y, -z+1$]. The W_3Cu_3 rectangle contains Cu(3) as well as Cu(4) moieties of short and almost linear equatorial CN bridge [Cu(4)–N(12), 1.944(19) Å; Cu(4)–N(12)–C(12), 172.1(17)°] and two significantly longer and strongly bent axial bridges [Cu(4)–N(22), 2.287(16) Å; Cu(4)–N(22)–C(22), 149.9(18)°; Cu(4)–N(28c), 3.114(19) Å; Cu(4)–N(28c)–C(28c), 148.4°] [symmetry operation: (c) $x-1, y, z$]. These metric parameters show that cyano bridges within W_2Cu_2 symmetry independent unit are much shorter than the cyano bridges between the units. The terminal cyano ligands of $[W(CN)_8]^{4-}$ and the terminal amino arms of the tetren ligand are presumably involved in the hydrogen bonding interaction, which link parallel chains to the lattice water molecules.

Both compounds: $[Cu^{II}(tetrenH_2)]_2[W^{IV}(CN)_8]_2 \cdot 5H_2O$, **1**, and $[Cu^{II}(tetrenH_2)][Cu^{II}(tetrenH)][W^{IV}(CN)_8][W^{IV}(CN)_8] \cdot 2.5H_2O$, **2**, obtained under different pH conditions are constructed from the same precursors, but the assemblies have a different superstructure. The preference for either supramolecular assembly can be attributed to the redox properties of W(v)/W(IV) and Cu(III)/Cu(II) couples along with substitutional reactivity of the $[Cu(tetren)]^{2+}$ complex at different pHs stabilised by supramolecular H-bonding interactions.

$[Cu^{II}(dien)][W^{IV}(CN)_8] \cdot 4H_2O$, **3**. Selected bond lengths and angles are listed in Table 4. The structure is built of 2-D strongly folded layers consisting of W(IV) and Cu(II) centres joined by cyano bridges and water molecules of crystallization located within the layer (Fig. 6a). The layers form a square grid pattern with tungsten atoms in the corners and $-CN-Cu(dien)-$

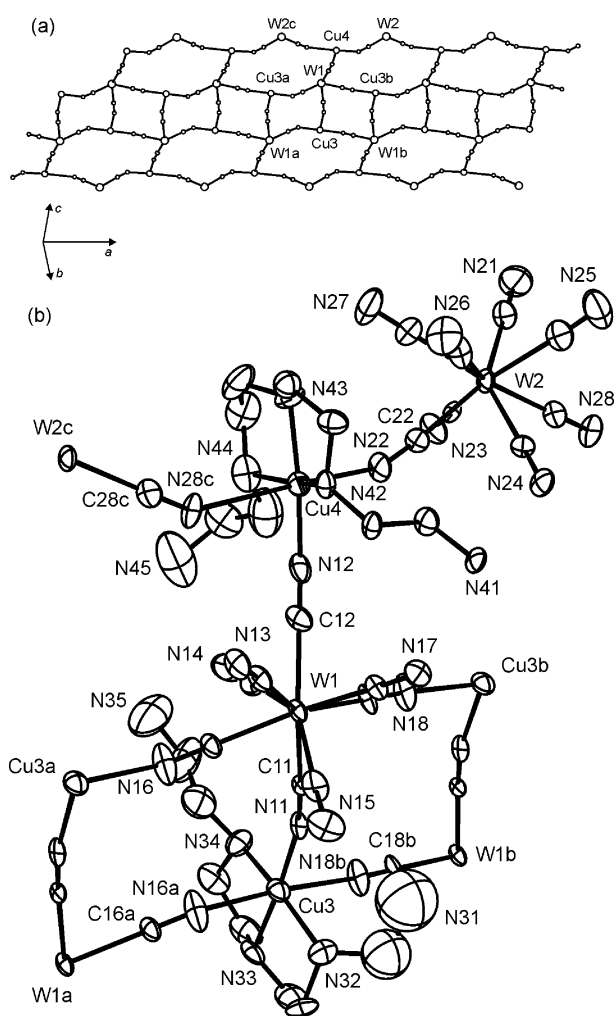


Fig. 5 Crystal structure of **2**: (a) cyano-bridged skeleton (only W and Cu centres and CN⁻ bridging ligands are shown), (b) an ORTEP drawing, in which selected atoms are numbered, showing cyano-bridged W₂Cu₂ units [symmetry equivalent operations: (a) $1 - x, -y, 1 - z$; (b) $x - 1, -y, -z + 1$; (c) $x - 1, y, z$]. All atoms are represented by 30% probability ellipsoids. Hydrogen and oxygen atoms are omitted for clarity.

NC- linkages on the edges of the squares of 4,4 topology.^{2a} Each strongly folded layer resembles an egg box.

Fig. 6b depicts the local environment of the constituents of the compound. Each octacyanotungstate unit reveals a square antiprismatic geometry coordinated to four cyano bridges of two different geometries and to four terminal cyano ligands. The mean values of the W–C and C–N bond lengths and W–C–N angles (2.16, 1.15 Å and 177°, respectively) in [W(CN)₈]⁴⁻ are typical for ionic and bridged compounds based on octacyanotungstates. The copper centre adopts a distorted square pyramidal geometry. The dien ligand with typical Cu–N bond lengths slightly greater than 2.0 Å is coordinated at three equatorial sites. The remaining fourth equatorial and one axial position are occupied by N atoms of cyano-bridges of two different geometries. The equatorial bridge is shorter (Cu(1)–N(4) 1.947(3) Å) and less bent (Cu(1)–N(4)–C(4) 161.2(4)°) than the axial one (Cu(1a)–N(1) 2.290(3) Å and Cu(1a)–N(1)–C(1) 140.7(3)°) [symmetry equivalent operation: (a) $-x + 1/2, y - 1/2, -z$].

The lattice water molecules are involved in the extensive hydrogen bonding system (Fig. 7 and Table S1†). O1 atoms of the lattice water are located in the external areas of the layers and linked to the terminal cyano ligands of two neighbouring layers. O2 atoms are situated in the internal part of the layers, bonding with terminal and bridging cyano ligands as well as RNH₂ groups from the dien ligand. Generally, the extensive

Table 4 Selected bond lengths (Å) and angles (°) for [Cu^{II}(dien)]₂[W^{IV}(CN)₈]⁴⁻·4H₂O, **3**, and [Cu^{II}(dien)]₂[Mo^{IV}(CN)₈]⁴⁻·4H₂O, **4**

[Cu ^{II} (dien)] ₂ [W ^{IV} (CN) ₈] ⁴⁻ ·4H ₂ O, 3			
<i>W(1)</i>			
W(1)–C(1)	2.161(3)	C(1)–N(1)	1.151(4)
W(1)–C(2)	2.162(3)	C(2)–N(2)	1.149(5)
W(1)–C(3)	2.162(3)	C(3)–N(3)	1.146(5)
W(1)–C(4)	2.143(3)	C(4)–N(4)	1.153(4)
<i>Cu(1)</i>			
Cu(1a)–N(1)	2.290(3)	Cu(1a)–N(1)–C(1)	140.7(3)
Cu(1)–N(4)	1.947(3)	Cu(1)–N(4)–C(4)	161.2(4)
[Cu ^{II} (dien)] ₂ [Mo ^{IV} (CN) ₈] ⁴⁻ ·4H ₂ O, 4			
<i>Mo(1)</i>			
Mo(1)–C(1)	2.157(2)	C(1)–N(1)	1.151(4)
Mo(1)–C(2)	2.161(3)	C(2)–N(2)	1.149(4)
Mo(1)–C(3)	2.162(3)	C(3)–N(3)	1.155(4)
Mo(1)–C(4)	2.149(2)	C(4)–N(4)	1.147(3)
<i>Cu(1)</i>			
Cu(1a)–N(1)	2.291(2)	Cu(1a)–N(1)–C(1)	140.7(2)
Cu(1)–N(4)	1.949(2)	Cu(1)–N(4)–C(4)	161.5(3)

Symmetry equivalent operation: (a) $-x + 1/2, y - 1/2, -z$.

network of hydrogen bonds penetrates the layer to stabilize its geometry and join the adjacent layers into the 3-D architecture. The molybdenum analogue [Cu^{II}(dien)]₂[Mo^{IV}(CN)₈]⁴⁻·4H₂O, **4**, was found to be isomorphous.

Cyanide stretching frequencies

Values of ν_{CN} for the bridged assemblies are presented together with related data in Table 5.^{1a,e,g,h,m-o,37–45} The range and pattern of ν_{CN} bands is sensitive to the coordination geometry of the [W(CN)₈]⁴⁻ precursor, interactions with counterions and packing pattern in the crystal lattice as well as to the presence of bridging CN⁻ ligands. The bridging ν_{CN} values are controlled by (i) the dominating kinematic effect, which results in constraints on the motion of CN⁻ and is expected to increase ν_{CN} ; and (ii) complex electronic and bridge geometric factors.⁴⁶

The infrared spectrum of [Cu^{II}(tetrenH₂)]₂[W^{IV}(CN)₈]⁴⁻·8H₂O, 1·3H₂O, in the range 2095–2128 cm⁻¹ displays stretching bands consistent with terminal cyano ligands from a [W(CN)₈]⁴⁻ of distorted DD geometry, whereas the bands at 2151 and 2160 cm⁻¹ can be safely assigned to bridging ν_{CN} modes.

The [Cu^{II}(tetrenH₂)]₂[Cu^{II}(tetrenH)]₂[W^V(CN)₈]³⁻·13H₂O, 2·10.5H₂O, is characterised by the ν_{CN} bands at 2115m,br, 2143w(sh), 2156m,br and 2180w(sh) cm⁻¹. Taking into account the range and pattern of the [W^V(CN)₈]³⁻ and [W^{IV}(CN)₈]⁴⁻ bands, we assign the IR ν_{CN} pattern of 2·10.5H₂O to the superposition of high-intensity W(IV) and low-intensity W(V) cyano stretching vibrations in W cyano-bridged linkages (Fig. S2†).

The ν_{CN} stretching pattern of the [W(CN)₈]⁴⁻ unit in [Cu^{II}(dien)]₂[W^{IV}(CN)₈]⁴⁻·4H₂O, **3**, contains the bands at 2112 and 2131 cm⁻¹, which are assigned to terminal CN⁻ ligands and that at 2157 cm⁻¹ assigned to bridging CN⁻ ligands. The infrared spectrum of [Cu^{II}(dien)]₂[Mo^{IV}(CN)₈]⁴⁻·4H₂O, **4**, exhibits ν_{CN} bands at 2112 and 2132 cm⁻¹ assigned to terminal cyano ligands, whereas the stretching band of the bridging cyano ligands is seen at 2157 cm⁻¹.

Magnetic properties

The magnetic susceptibilities of **1–3** have been measured in a temperature range of 4.2–250 K under the applied field of 5 kOe. It was checked at $T = 4.2$ K that susceptibility did not

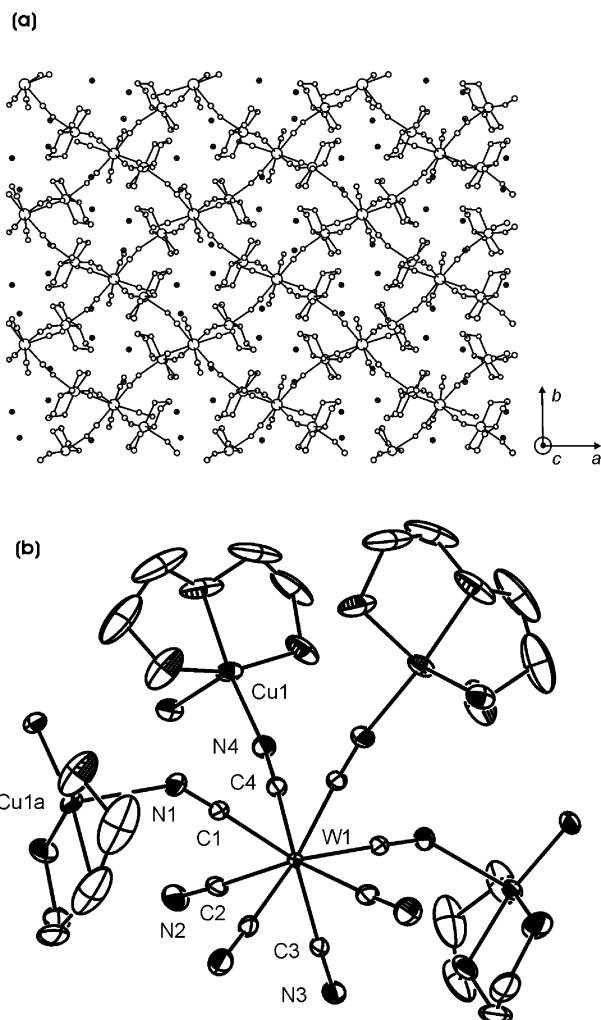


Fig. 6 Crystal structure of **3**: (a) representative view of the polymeric layer and (b) ORTEP drawing with selected atoms numbering scheme showing cyano-bridged W_2Cu_2 square units [symmetry equivalent operation: (a) $-x + 1/2, y - 1/2, -z$]. All atoms are represented by 30% probability ellipsoids. Hydrogen and oxygen atoms are omitted for clarity. For clarity, the disordered carbon and nitrogen atoms of dien ligand are presented with average ellipsoids.

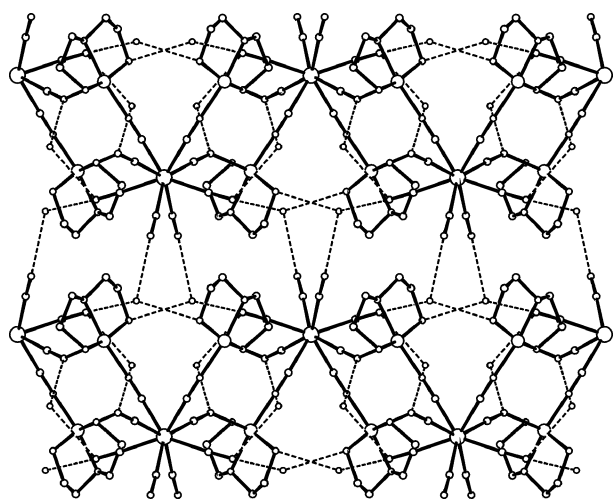


Fig. 7 3-D hydrogen bonded network in **3** and **4**; view along b crystallographic direction.

depend on the value of the applied field. The curve $\chi(T)$ for **1**· $3H_2O$ obeys the Curie–Weiss law in the range 4.2–250 K with the negative Weiss constant of $\theta = -0.33$ K (± 0.07) K and $C = 0.90$ (± 0.01) cm^3 K mol $^{-1}$ per Cu_2W_2 formula unit. The

Curie constant C is slightly larger than the expected spin-only value of $C = 0.75$ cm^3 K mol $^{-1}$ calculated for two magnetically isolated $Cu(II)$ ($S = 1/2$) with $g = 2.00$. The field dependence of magnetization for **1**· $3H_2O$, measured at $T = 4.3$ K is shown in Fig. 8. It is seen that the observed magnetization (per Cu_2W_2) agrees well with the value predicted from the Brillouin function for two independent $Cu(II)$ centres in the range of the applied field of 0–60 kOe.

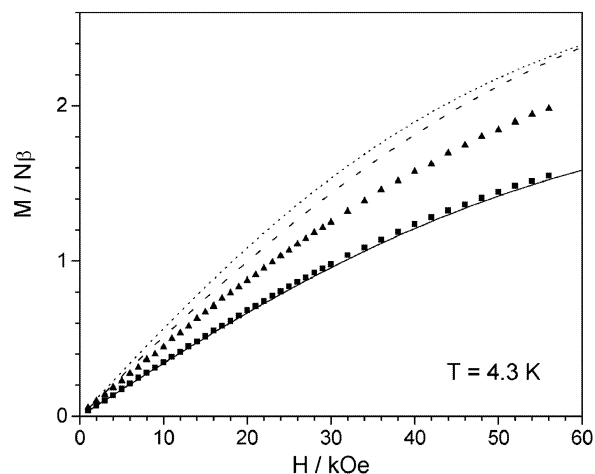


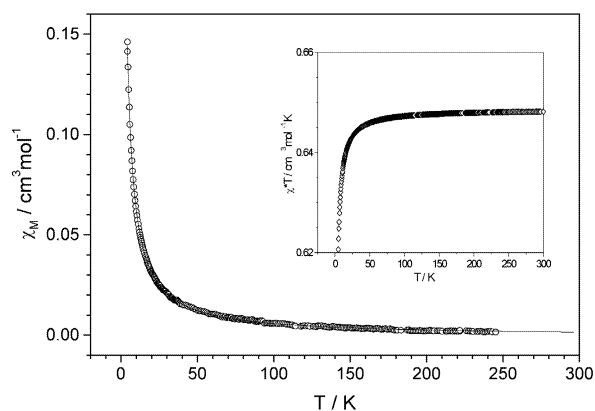
Fig. 8 The field dependence of magnetisation for **1**· $3H_2O$ (■) and **2**· $10.5H_2O$ (▲) at $T = 4.3$ K and the sum of calculated Brillouin functions for two isolated spins $S = 1/2$ (—), three isolated spins $S = 1/2$ (-.-) and for isolated spins $S = 1$ and $1/2$ (···).

The curve $\chi(T)$ for **2**· $10.5H_2O$ in the range 4.2–250 K obeys the Curie–Weiss law with a negative Weiss constant $\theta = -0.78$ (± 0.1) K, and $C = 1.30$ (± 0.2) cm^3 K mol $^{-1}$ per Cu_2W_2 formula unit which is larger than the expected spin-only value $C = 1.125$ cm^3 K mol $^{-1}$ calculated for 3 isolated spins of $S = 1/2$ assuming $g = 2.00$. This result shows that, besides the two $Cu(II)$ centres of $S = 1/2$, the additional spin $S = 1/2$ per formula unit is present, which we formally ascribe to $[W^V(CN)_8]^{3-}$. The value obtained for the Curie constant C is not much less than the $C = 1.375$ expected for the case of $S = 1$ and $1/2$. Therefore, we assume the model of a weak ferromagnetic interaction between two paramagnetic centres Cu^{II} and W^V isolated by diamagnetic $[W^{IV}(CN)_8]^{4-}$ spacer from another Cu^{II} centre within the W^V – CN – Cu^{II} – NC – W^{IV} – CN – Cu^{II} unit with short cyano bridges linked by significantly longer cyano bridges into the 1-D network (Fig. 5). An extremely weak increase of χ^*T (Fig. S3†) upon cooling is observed followed by a steep decrease below ca. 70 K when the stronger antiferromagnetism comes into play. The field dependence of magnetization for **2**· $10.5H_2O$, measured at 4.3 K is shown in Fig. 8. The experimental data can be compared to the Brillouin function calculated for (i) three isolated $S = 1/2$ spins with $g = 2.00$ and for (ii) the sum of one resultant spin $S = 1$ and one spin $S = 1/2$. It can be seen that the observed magnetization (per Cu_2W_2) is weaker, as an indication of the antiferromagnetic interaction between Cu^{II} – W^V units, which can not be neglected at $T = 4.3$ K.

The curve $\chi(T)$ in the range 4.2–250 K for **3** obeys the Curie–Weiss law with small negative Weiss constant $\theta = -0.2$ (± 0.04) K and $C = 0.65$ (± 0.01) cm^3 K mol $^{-1}$ per Cu_2W^{IV} formula unit. The C value is slightly lower than the expected spin-only value of $C = 0.68$ calculated for 2 magnetically isolated $Cu(II)$ centres ($S = 1/2$) assuming $g = 2.1$. Fig. 9 gives the $\chi(T)$ plot for **3** together with the inset showing the temperature dependence of the χ^*T product. The χ^*T dependence indicates that **3** behaves like a simple paramagnet, where paramagnetic $Cu(II)$ centres are isolated by the diamagnetic $[W^{IV}(CN)_8]^{4-}$ spacer. Weak antiferromagnetic interactions become visible at low temperatures.

Table 5 Cyanide stretching frequencies of the 1–4 assemblies and literature references

Ionic compounds	$\nu_{\text{CN}}/\text{cm}^{-1}$	Ref.
$\text{K}_4[\text{W}^{\text{IV}}(\text{CN})_8]\cdot 2\text{H}_2\text{O}$	2138w, 2130vs, 2128vw, 2125vs, 2114vw, 2110vw, 2101m(sh), 2095vs	37, 38
$\text{Ti}_4[\text{W}^{\text{IV}}(\text{CN})_8]$	2134w, 2123w, 2118sh, 2115m, 2104s, 2100vs, 2098s,sh, 2088s, 2079s,sh, 2075vs	38
$(4,4'\text{-bpyH}_2)_2[\text{W}^{\text{IV}}(\text{CN})_8]$	2105vs, 2117sh	39
$(2,2'\text{-bpyH}_2)_2[\text{W}^{\text{IV}}(\text{CN})_8]$	2140s, 2118vs	40
$(\text{dq})_2[\text{W}^{\text{IV}}(\text{CN})_8]\cdot 5\text{H}_2\text{O}$	2117vs, 2095vs, 2057w	41
$[\text{Pt}(\text{NH}_3)_4]_2[\text{W}^{\text{IV}}(\text{CN})_8]$	2138vw, 2129vw, 2124vw, 2113s, 2098vs, 2071w, 2057w	42
$\text{Na}_3[\text{W}^{\text{V}}(\text{CN})_8]\cdot 4\text{H}_2\text{O}$	2170m, 2164m, 2160vs, 2154vs, 2146m, 2144m	43
$\text{K}_3[\text{W}^{\text{V}}(\text{CN})_8]\cdot 1.5\text{H}_2\text{O}$	2162w, 2159m, 2151vs, 2148vs	43
$(\text{Bu}_4\text{N})_3[\text{W}^{\text{V}}(\text{CN})_8]\cdot \text{H}_2\text{O}$	2140s, 2130vs	43
Bridged assemblies		
$[\text{Cu}^{\text{II}}(\text{tetrenH}_2)]_2[\text{W}^{\text{IV}}(\text{CN})_8]_2\cdot 8\text{H}_2\text{O}, 1\cdot 3\text{H}_2\text{O}$	(2160, 2151)w, 2128m, (2107, 2101, 2095)s	This work
$[\text{Cu}^{\text{II}}(\text{tetrenH}_2)]_2[\text{Cu}^{\text{II}}(\text{tetrenH})][\text{W}^{\text{V}}(\text{CN})_8][\text{W}^{\text{IV}}(\text{CN})_8]_2\cdot 13\text{H}_2\text{O}, 2\cdot 10.5\text{H}_2\text{O}$	2180w(sh), 2156m, 2143w(sh), 2115m	This work
$[\text{Cu}^{\text{II}}(\text{dien})]_2[\text{W}^{\text{IV}}(\text{CN})_8]\cdot 4\text{H}_2\text{O}, 3$	2157s, 2131s(sh), 2112m	This work
$[\text{Cu}^{\text{II}}(\text{dien})]_2[\text{Mo}^{\text{IV}}(\text{CN})_8]\cdot 4\text{H}_2\text{O}, 4$	2157s, 2132s(sh), 2112m	This work
$\text{Mn}_2[\text{Mo}^{\text{IV}}(\text{CN})_8]\cdot 8\text{H}_2\text{O}$	2161sh, 2145sh, 2128vs(br)	44
$\text{Mn}_2[\text{Mo}^{\text{IV}}(\text{CN})_8]$	2174m(br), 2131w(br), 2090s(br)	44
$\text{Fe}_2[\text{Mo}^{\text{IV}}(\text{CN})_8]\cdot x\text{H}_2\text{O}$	2137m(br)/2134	1g, 44
$\text{Co}_2[\text{Mo}^{\text{IV}}(\text{CN})_8]\cdot 9\text{H}_2\text{O}$	2141m, 2118(sh)	44
$\text{Ni}_2[\text{Mo}^{\text{IV}}(\text{CN})_8]\cdot 9\text{H}_2\text{O}$	2157s, 2110(sh)	44
$\text{Cu}_2[\text{Mo}^{\text{IV}}(\text{CN})_8]\cdot x\text{H}_2\text{O}$	2166s(br)/2162(br)/2161(br)	1h, 4, 44
$\text{H}_4[\text{Mo}^{\text{IV}}(\text{CN})_8]\cdot 8\text{H}_2\text{O}$	2160, 2130, 2090	44
$(\text{UO}_2)[\text{Mo}^{\text{IV}}(\text{CN})_8]\cdot 6\text{-}8\text{H}_2\text{O}$	2140s(br)	45
$[(\text{Me}_3\text{Sn})_4][\text{Mo}^{\text{IV}}(\text{CN})_8]$	2143s, 2105(sh)	1a
$[(\text{Me}_3\text{Sn})_4][\text{W}^{\text{IV}}(\text{CN})_8]$	2141s, 2105(sh)	1a
$[\text{Mn}(\text{bpy})_2]_2[\text{Mo}^{\text{IV}}(\text{CN})_8]\cdot 8\text{H}_2\text{O}$	2150m, 2138vs, 2119vs, 2110vs, 2069w	1m
$[\text{Mn}(\text{bpy})_2]_2[\text{W}^{\text{IV}}(\text{CN})_8]\cdot 14\text{H}_2\text{O}$	2147m, 2124(sh), 2108vs	1m
$[\text{Cu}(\text{bpy})_2]_2[\text{Mo}^{\text{IV}}(\text{CN})_8]\cdot 5\text{H}_2\text{O}\cdot \text{MeOH}$	2124, 2112	1h
$\text{Cs}_2[\text{Pt}(\text{en})_2\text{Cl}_2]\{\text{Pt}(\text{en})_2[\text{Mo}^{\text{IV}}(\text{CN})_8]_2\cdot 10\text{H}_2\text{O}$	2151s, 2133s, 2124s, 2114s, 2107s	32
$[\text{Mn}_2\text{L}_2(\text{H}_2\text{O})][\text{Mo}^{\text{IV}}(\text{CN})_8]\cdot 5\text{H}_2\text{O}$	2121, 2103	1e
$\{\mu\text{-}(\text{bpym})[\text{Mn}(\text{H}_2\text{O})]_2\text{-}\mu\text{-}(\text{NC})_6\text{Mo}^{\text{IV}}(\text{CN})_2\}$	2161m, 2118s	1n
$\{\mu\text{-}(\text{bpym})[\text{Mn}(\text{H}_2\text{O})]_2\text{-}\mu\text{-}(\text{NC})_6\text{W}^{\text{IV}}(\text{CN})_2\}$	2160m, 2112s	1n
$\{\text{Cu}_{1.5}[\text{Mo}^{\text{V}}(\text{CN})_8]\cdot 3\text{H}_2\text{O}\}_n$	2236, 2201	4
$\{\text{Mn}_6(\text{H}_2\text{O})_9[\text{W}^{\text{V}}(\text{CN})_8]_4\cdot 13\text{H}_2\text{O}\}_n$	2196, 2172, 2160sh, 2140sh	1d
$[\text{Cu}(\text{tn})_3][\text{W}^{\text{V}}(\text{CN})_8]_2\cdot 3\text{H}_2\text{O}$	2189m, 2150s	1o
$[\text{Cu}(\text{pn})_3][\text{W}^{\text{V}}(\text{CN})_8]_2\cdot 3\text{H}_2\text{O}$	2203s, 2188s, 2156s	1o
$(\text{tetrenH}_5)_{0.8}[\text{CuW}^{\text{V}}(\text{CN})_8]_4\cdot 7.2\text{H}_2\text{O}\}_n$	2201m, 2164s	7

**Fig. 9** The temperature dependence of molar magnetic susceptibility for **3** with the best fit of the Curie–Weiss law. Inset: the temperature dependence of $\chi T(T)$.

Very recently, Tang and co-workers⁴⁷ have produced the complex $\{[\text{Cu}^{\text{II}}(\text{dien})]_2[\text{W}^{\text{IV}}(\text{CN})_8](\text{OH})\cdot 3\text{H}_2\text{O}\}_4$ at pH 9 with the same structural data as for $[\text{Cu}^{\text{II}}(\text{dien})]_2[\text{W}^{\text{IV}}(\text{CN})_8]\cdot 4\text{H}_2\text{O}$, **3**. The authors have reported also its ν_{CN} stretching frequencies corresponding well with these of **3**. In contrast to **3**, the compound shows magnetic behaviour characteristic of weak ferromagnetic coupling between the Cu(II) and W(V) ions with a weak intermolecular antiferromagnetic interaction at low tem-

perature. In view of the different magnetic properties of **3** and the Tang complex, the two compounds can be considered as two different phases.

ESR spectra

The representative X band ESR spectra of **1**·3H₂O and **2**·10.5H₂O at 77 K are presented in Fig. S4.† The ESR spectrum of **1**·3H₂O consists of two superimposing signals with axial symmetry (simulated parameters for centre 1: $g_{\parallel} = 2.087$, $g_{\perp} = 2.047$; centre 2: $g_{\parallel} = 2.309$, $g_{\perp} = 2.096$). These results indicate that **1**·3H₂O contains two different, axially elongated octahedral and square pyramidal Cu(II) centres,^{21,22,48} conforming to the crystal structure and magnetic data. The centre 1 is therefore assigned to octahedral Cu(2), while the centre 2 is assigned to square pyramidal Cu(1). The ESR spectrum for **2**·10.5H₂O was simulated as a one signal with rhombic symmetry ($g_1 = 2.160$, $g_2 = 2.041$, $g_3 = 2.036$). The signal of the large line width is consistent with the presence of Cu(II) centres of strongly distorted octahedral geometry, undistinguishable by ESR. There is no observable signal of $[\text{W}^{\text{V}}(\text{CN})_8]^{3-}$ ^{43,49} in **2**·10.5H₂O on the ESR timescale. The ESR spectra are inconsistent with the valence-trapped description of $[\text{Cu}^{\text{II}}(\text{tetrenH}_2)]_2[\text{Cu}^{\text{II}}(\text{tetrenH})][\text{W}^{\text{V}}(\text{CN})_8][\text{W}^{\text{IV}}(\text{CN})_8]\cdot 13\text{H}_2\text{O}$, **2**·10.5H₂O. These observations can be explained in terms of delocalisation of the spin density over the whole polymeric structure due to plausible $\text{Cu}^{\text{II}}\text{W}^{\text{V}} \leftrightarrow \text{Cu}^{\text{III}}\text{W}^{\text{IV}}$ electron transfer process. In such a case the large broadening of the line might lead to the disappearance of the ESR signal.

Conclusions

We have demonstrated the use of aliphatic polyamine copper(II) tectons with [N₃] donor atom sets in the crystal engineering of coordination polymers based on [W(CN)₈]^{3-/4-} precursors. Introduction of [Cu(tetrenH₂)(H₂O)₂]⁴⁺ and [Cu(dien)(H₂O)₂]²⁺ building blocks leads to the construction of 1-D and 2-D coordination polymers of different topologies. The self-assembly of [Cu^{II}(tetrenH₂)₂][W^{IV}(CN)₈]₂·5H₂O, **1**, and [Cu^{II}(tetrenH₂)][Cu^{II}(tetrenH)][W^V(CN)₈][W^{IV}(CN)₈]₂·2.5H₂O, **2**, is controlled by the redox properties of W(v)/W(IV) and Cu(III)/Cu(II) couples along with substitutional reactivity of the [Cu(tetren)]²⁺ complex at different pH.

The structures of **1–4** indicate that the stereochemical characteristics of the aliphatic polyamine copper(II) tectons with [N₃] donor atom sets may be exploited to organize the coordinative CN- and H-bonding interactions in the supramolecular structures.

The 5- and 6-coordinate copper moieties generate coordination polymers: 1-D **1** and **2**. While penta-coordinated Cu(II) corners are sufficient to form a 0-D W₂Cu₂ square, the extension into the 1-D polymeric structures is due to the ability of the copper centres to possess hexa-coordinated geometry, which enables the creation of an additional cyano bridge leading to *mer*-[Cu(tetrenH₂)(NC)₃] moieties. Detached terminal N atoms of tetren ligand in either [Cu(tetrenH₂)(NC)₂] or *mer*-[Cu(tetrenH₂)(NC)₃] seem to provide a steric hindrance and prevent the construction of higher dimensionality polymer, contrary to the case of [Cu(dien)(H₂O)₂]²⁺ tecton. When the square pyramidal [Cu(dien)(H₂O)₂]²⁺ reacts with octacyano-metalates(IV), self-assembly leads to the formation of 2-D compounds [Cu^{II}(dien)₂][M^{IV}(CN)₈]₂·4H₂O that crystallise in a square grid pattern with tungsten atoms in the corners and –CN–Cu(dien)–NC– linkages on the edges of the squares.

Acknowledgements

This work was partially supported by Jagiellonian University and Tempus JEP12236-97.

References

- (a) J. Lu, W. T. A. Harrison and A. J. Jacobson, *Angew. Chem., Int. Ed.*, 1995, **34**, 2557; (b) Z. J. Zhong, H. Seino, Y. Mizobe, M. Hidai, A. Fujishima, S. Ohkoshi and K. Hashimoto, *J. Am. Chem. Soc.*, 2000, **122**, 2952; (c) J. Larionova, M. Gross, M. Pilkington, H. Andres, H. Stoeckli-Evans, H. Güdel and S. Decurtins, *Angew. Chem., Int. Ed.*, 2000, **39**, 1605; (d) Z. J. Zhong, H. Seino, Y. Mizobe, M. Hidai, M. Verdager, S. Ohkoshi and K. Hashimoto, *Inorg. Chem.*, 2000, **39**, 5095; (e) G. Rombaut, S. Golhen, L. Ouahab, C. Mathonière and O. Kahn, *J. Chem. Soc., Dalton Trans.*, 2000, 3609; (f) A. K. Sra, G. Rombaut, F. Lahitête, S. Golhen, L. Ouahab, C. Mathonière, J. V. Yakhmi and O. Kahn, *New J. Chem.*, 2000, **24**, 871; (g) G. Rombaut, C. Mathonière, P. Guionneau, S. Golhen, L. Ouahab, M. Verelst and P. Lecante, *Inorg. Chim. Acta*, 2001, **326**, 27; (h) G. Rombaut, M. Verelst, S. Golhen, L. Ouahab, C. Mathonière and O. Kahn, *Inorg. Chem.*, 2001, **40**, 1151; (i) S. Ohkoshi and K. Hashimoto, *J. Photochem. Photobiol. C: Photochem. Rev.*, 2001, **2**, 71; (j) D. Li, S. Gao, L. Zheng, W. Sun, T. Okamura, N. Ueyama and W. Tang, *New J. Chem.*, 2002, **26**, 485; (k) D. Li, T. Okamura, W. Sun, N. Ueyama and W. Tang, *Acta Crystallogr., Sect. C*, 2002, **58**, m280; (l) B. Sieklucka, J. Szklarzewicz, T. J. Kemp and W. Errington, *Inorg. Chem.*, 2000, **34**, 2557; (m) R. Podgajny, C. Desplanches, B. Sieklucka, R. Sessoli, V. Villar, C. Paulsen, W. Wernsdorfer, Y. Dromzée and M. Verdager, *Inorg. Chem.*, 2002, **41**, 1323; (n) J. M. Herrera, D. Armentano, G. de Munno, F. Lloret, M. Julve and M. Verdager, *New J. Chem.*, 2003, **27**, 128; (o) D. F. Li, L. Zheng, X. Wang, J. Huang, S. Gao and W. Tang, *Chem. Mater.*, 2003, **15**, 2094.
- (a) S. R. Batten and R. Robson, *Angew. Chem., Int. Ed.*, 1998, **37**, 1460; (b) M. J. Zaworotko, *Chem. Commun.*, 2001, 1; (c) B. J. Holliday and Ch. A. Mirkin, *Angew. Chem., Int. Ed.*, 2001, **40**, 2022; (d) B. Moulton and M. J. Zaworotko, *Chem. Rev.*, 2001, **101**, 1629; (e) S. R. Batten, *Solid State Mater. Sci.*, 2001, **5**, 107; (f) S. R. Batten, *CrystEngComm*, 2001, **18**, 1; (g) Ch. A. Hunter and J. K. M. Sanders, *J. Am. Chem. Soc.*, 1990, **112**, 5525; (h) H. Krass, E. A. Plummer, J. M. Heider, Ph. R. Barker, N. W. Alcock, Z. Pikramenou, M. J. Hannon and D. G. Kurth, *Angew. Chem., Int. Ed.*, 2001, **40**, 3862; (i) J. Lu, A. Mondal, B. Moulton and M. J. Zaworotko, *Angew. Chem., Int. Ed.*, 2001, **40**, 2113; (j) P. J. Nichols, C. L. Raston and J. W. Steed, *Chem. Commun.*, 2001, 1062; (k) J. W. Steed and J. L. Atwood, in *Supramolecular Chemistry*, J. Wiley & Sons, Chichester, 2000, ch. 1, pp. 19–30, ch. 7, pp. 390–392.
- (a) E. L. Muetterties, *Inorg. Chem.*, 1973, **12**, 1963; (b) J. K. Burdett, R. Hoffmann and R. C. Fay, *Inorg. Chem.*, 1978, **17**, 2553; (c) J. G. Leipoldt, S. S. Basson and A. Roodt, *Adv. Inorg. Chem.*, 1993, **40**, 241; (d) J. G. Leipoldt, S. S. Basson, A. Roodt and W. Purcell, *Polyhedron*, 1992, **11**, 2277.
- Sh. Ohkoshi, N. Machida, Zh. J. Zhong and K. Hashimoto, *Synth. Met.*, 2001, **122**, 523.
- W. Meske and D. Babel, *Z. Naturforsch., Teil B*, 1999, **54**, 117.
- R. Podgajny, C. Desplanches, F. Fabrizi De Biani, B. Sieklucka, Y. Dromzée and M. Verdager, to be published.
- R. Podgajny, T. Korzeniak, M. Bałanda, T. Wasiutynski, W. Errington, T. J. Kemp, N. W. Alcock and B. Sieklucka, *Chem. Commun.*, 2002, 1138.
- R. Podgajny, R. Kania, T. Korzeniak, Y. Dromzée, W. Errington, K. Lewinski, K. Stadnicka, C. Desplanches, M. Bałanda, J. Wasiutynski, T. J. Kemp, M. Verdager and B. Sieklucka, *20th European Crystallographic Meeting ECM 20*, Book of Abstracts, "EJB" Publisher, Kraków, Poland, 2001, p. 343.
- (a) J. G. Leipoldt, L. D. C. Bok and P. J. Z. Cilliers, *Z. Anorg. Allg. Chem.*, 1974, **350**, 409; (b) A. Samotus, *Pol. J. Chem.*, 1973, **47**, 265.
- (a) B. Sieklucka, A. Kanas and A. Samotus, *Transition Met. Chem.*, 1982, **7**, 131; (b) B. Sieklucka and A. Samotus, *J. Photochem. Photobiol. A: Chem.*, 1993, **74**, 115.
- M. K. Urtiaga, M. I. Arriortua, R. Cortes and T. Rojo, *Acta Crystallogr., Sect. C*, 1996, **52**, 3007.
- G. P. Lozos, B. M. Hoffman and C. G. Franz, Sim14A Program, Chemistry Department, Northwestern Department, IL, QCPE, no. 265.
- R. Binstead and A. Zuberbühler, SPECFIT – A Program for Fitting Equilibrium and Kinetic Systems, 1993–1998, Spectrum Software Associates, Marlborough, MA, USA.
- G. M. Sheldrick, SHELXS-86, Program for the solution of crystal structures, University of Göttingen, Federal Republic of Germany, 1986.
- D. J. Watkin, J. R. Carruthers and P. W. Betteridge, *Crystals User Guide*, Chemical Crystallography Laboratory, University of Oxford, Oxford, UK, 1988.
- D. T. Cromer, *International Tables for X-ray Crystallography*, Kynoch, Birmingham, UK, 1974, vol. IV.
- Z. Otwinowski and W. Minor, COLLECT, Nonius BV, Delft, The Netherlands, 1997–2000.
- Z. Otwinowski and W. Minor, *Methods Enzymol.*, 1997, **276**, 307.
- A. Altomare, G. Cascarano, C. Giacovazzo and A. Gualardi, *J. Appl. Crystallogr.*, 1993, **26**, 343.
- (a) G. M. Sheldrick, SHELXS-97, Program for the solution of crystal structures, University of Göttingen, Germany, 1997; (b) G. M. Sheldrick, SHELXL-97, Program for the refinement of crystal structures, University of Göttingen, Germany, 1997; G. M. Sheldrick, SHELXTL/PC, Siemens Analytical X-Ray Instruments, Madison, WI, 1994.
- M. Duggan, N. Ray, B. Hathaway, G. Tomlinson, P. Brint and K. Pelin, *J. Chem. Soc., Dalton Trans.*, 1980, 1342.
- Z. Lu, Ch. Duan, Y. Tian, X. You and X. Huang, *Inorg. Chem.*, 1996, **35**, 2253.
- A. M. Dittler-Klingemann, Ch. Orvig, F. E. Hahn, F. Thaler, C. D. Hubbard, R. van Eldik, S. Schindler and I. Fábian, *Inorg. Chem.*, 1996, **35**, 7798.
- B. Kurzak, D. Kroczevska and J. Jezierska, *Polyhedron*, 1998, **17**, 1831.
- R. J. Deeth and M. Gerloch, *Inorg. Chem.*, 1984, **23**, 3846.
- A. B. P. Lever, *Inorganic Electronic Spectroscopy*, Elsevier, Amsterdam, 2nd edn., 1984, ch. 6, p. 557.
- H. B. Jonassen, J. A. Bertrand, F. R. Groves, Jr. and R. I. Stearns, *J. Am. Chem. Soc.*, 1957, **79**, 4279.
- H. B. Jonassen and L. Westermann, *J. Am. Chem. Soc.*, 1957, **79**, 4275.
- E. Colacio, J. M. Dominguez-Vera, M. Ghazi, R. Kivekäs, J. M. Moreno and A. Pajunen, *J. Chem. Soc., Dalton Trans.*, 2000, 505.
- F. Thétiot, S. Triki and J. S. Pala, *New J. Chem.*, 2000, **26**, 196.
- R. J. Parker, D. C. R. Hockless, B. Moubarakí, K. S. Murray and L. Spiccia, *Chem. Commun.*, 1996, 2789.

- 32 R. Podgajny, Y. Dromzée, K. Kruczała and B. Sieklucka, *Polyhedron*, 2001, **20**, 685.
- 33 H. Kou, D. Liao, P. Cheng, Z. Jiang, S. Yan, G. Wang, X. Yao and H. Wang, *J. Chem. Soc., Dalton Trans.*, 1997, 1503.
- 34 D. Fu, J. Chen, X. Tan, L. Jiang, S. Zhang, P. Zheng and W. Tang, *Inorg. Chem.*, 1997, **36**, 220.
- 35 F. Thétiot, S. Triki, J. Sala Pala, C. J. Gómez-García and S. Golhen, *Chem. Commun.*, 2002, 1078.
- 36 S. S. Basson, J. G. Leipoldt, L. D. C. Bok, J. S. van Vollenhoven and P. J. Cilliers, *Acta Crystallogr., Sect. B*, 1980, **36**, 1756.
- 37 T. Y. Long II and G. Vernon, *J. Am. Chem. Soc.*, 1971, **93**, 1919.
- 38 R. V. Parish, P. G. Simms, M. A. Wells and L. A. Woodward, *J. Chem. Soc. A*, 1968, 2882.
- 39 N. W. Alcock, A. Samotus and J. Szklarzewicz, *J. Chem. Soc., Dalton Trans.*, 1993, 885.
- 40 B. Nowicka, A. Samotus, J. Szklarzewicz, J. Burgess, J. Fawcett and D. R. Russel, *Transition Met. Chem.*, 1999, **24**, 177.
- 41 B. Nowicka, A. Samotus, J. Szklarzewicz, J. Burgess, J. Fawcett and D. R. Russel, *Polyhedron*, 1998, **17**, 3167.
- 42 R. Podgajny, B. Sieklucka, W. Łasocha, K. Stadnicka and H. Schenk, *Polyhedron*, 1999, **18**, 3527.
- 43 P. M. Kiernan and W. P. Griffith, *J. Chem. Soc., Dalton Trans.*, 1975, 2489.
- 44 G. F. McKnight and G. P. Haight, Jr., *Inorg. Chem.*, 1973, **12**, 3007.
- 45 M. Allen and S. J. Lippard, *Inorg. Chem.*, 1970, **9**, 991.
- 46 (a) K. Nakamoto, *Infrared and Raman Spectra of Inorganic and Coordination Compounds*, John Wiley and Sons, New York, 4th edn., 1986, ch. III-14, pp. 272–280; (b) C. A. Bignozzi, R. Argazzi, J. R. Schoonover, K. C. Gordon, R. B. Dyer and F. Scandola, *Inorg. Chem.*, 1992, **31**, 5260; (c) M. J. Scott and R. H. Holm, *J. Am. Chem. Soc.*, 1994, **116**, 11357; (d) M. A. Watzky, J. F. Endicott, X. Song, Y. Lei and A. Mccatangay, *Inorg. Chem.*, 1996, **35**, 3463; (e) K. R. Dunbar and R. A. Heintz, *Prog. Inorg. Chem.*, 1997, **45**, 283; (f) B. S. Lim and R. H. Holm, *Inorg. Chem.*, 1998, **37**, 4898; (g) A. Geiss and H. Vahrenkamp, *Eur. J. Inorg. Chem.*, 1999, 1793; (h) N. Richardson, U. Brand and H. Vahrenkamp, *Inorg. Chem.*, 1999, **38**, 3070; (i) Z. N. Chen, R. Appelt and H. Vahrenkamp, *Inorg. Chim. Acta*, 2000, **309**, 65; (j) A. Geiss and H. Vahrenkamp, *Inorg. Chem.*, 2000, **39**, 4029.
- 47 D. Li, S. Gao, L. Zheng, K. Yu and W. Tang, *New J. Chem.*, 2002, **26**, 1190.
- 48 M. K. Saha, D. K. Dey, B. Samanta, A. J. Edwards, W. Clegg and S. Mitra, *Dalton Trans.*, 2003, 488.
- 49 (a) B. Sieklucka, *J. Chem. Soc., Dalton Trans.*, 1997, 869; (b) R. Podgajny, B. Sieklucka and W. Łasocha, *J. Chem. Soc., Dalton Trans.*, 2000, 1799.